Available online at www.sciencedirect.com
SCIENCE DIRECT®
Journal of Sound and Vibration 273 (2004) 933–948
JOURNAL OF SOUND AND VIBRATION
www.elsevier.com/locate/jsvi

Exact solutions for the free vibrations of rectangular plates having in-plane moments acting on two opposite simply supported edges

Jae-Hoon Kang*, Hyun-Ju Shim

Department of Architectural Engineering, School of Architecture & Building Science, College of Engineering, Chung-Ang University, 221 Heuksuk-Dong Dongjak-Ku, Seoul 156-756, South Korea

Received 17 October 2002; accepted 10 May 2003

Abstract

An exact solution procedure is formulated for the free vibration analysis of rectangular plates having two opposite edges simply supported when these edges are subjected to linearly varying normal stresses causing pure in-plane moments. The other two edges may be clamped, simply supported or free, or they may be elastically supported. The transverse displacement (w) is assumed as sinusoidal in the direction of loading (x), and a power series is assumed in the lateral (y) direction (i.e., the method of Frobenius). Applying the boundary conditions yields the eigenvalue problem of finding the roots of a fourth order characteristic determinant. Care must be exercised to obtain adequate convergence for accurate vibration frequencies, as is demonstrated by two convergence tables. Some interesting and useful results for vibration frequencies and contour plots of their mode shapes are presented for plates having all nine possible combinations of clamped, simply supported or free unloaded edges. Particularly interesting is that for some of the edge conditions, applying opposite in-plane edge moments causes the fundamental frequency to increase initially.

1. Introduction

Transverse free vibrations of thin plates which are subjected to edge loads acting in their midplanes are areas of research which received a great deal of attention in the past century [1]. Most of the work has dealt with rectangular plates having uniformly distributed in-plane edge loads because the governing differential equations of motion have constant coefficients, yielding

*Corresponding author. Tel.: +82-2-820-5342; fax: +82-2-812-4150.
E-mail address: jhkang@cau.ac.kr (J.-H. Kang).

0022-460X/03/$ - see front matter
doi:10.1016/S0022-460X(03)00566-2

exact solutions for frequencies straightforwardly when two opposite edges of the plates are simply supported.

Of course, a plate may be loaded at two opposite edges by non-uniform, in-plane axial forces (N_x), the first variation from the uniform loading being one which varies linearly. A special case of this is a pure, in-plane bending moment. When the in-plane stresses vary throughout the plate the analysis is more formidable, and exact solutions are much more difficult to achieve. One finds few results for such plate vibration problems.

The present work derives exact solutions for the free vibration of a rectangular plate loaded at its simply supported edges by pure in-plane bending moments caused by normal stresses varying linearly along the edges. For the case of opposite edges being simply supported, a variables separable solution exists, which reduces the partial differential equation to an ordinary one having variable coefficients. This is solved by the classical power series method of Frobenius, and the convergence of the series is established for some representative cases. The present work presents novel, exact solutions for the free vibration frequencies and their corresponding mode shapes for all nine possible combinations of clamped, simply supported or free unloaded edges.

2. Analysis

A rectangular plate of thickness h, having lateral dimensions $a \times b$, is shown in Fig. 1. For purposes of description, a notation will be adopted as follows. The symbolism S–F–S–C, for example, will identify a rectangular plate with edges $x = 0,\ y = 0,\ x = a,\ y = b$ having simply supported, free, simply supported, and clamped boundary conditions. Two opposite edges ($x = 0$ and $x = a$) are simply supported, and are subjected to *in-plane* bending moments M caused by normal stresses σ_x which vary as

$$\sigma_x = -\sigma_0\left(1 - 2\frac{y}{b}\right), \tag{1}$$

where σ_0 is the tensile stress at $y = b$, as shown. The stress is related to the in-plane moment by

$$\sigma_0 = \frac{6M}{hb^2}. \tag{2}$$

The other two edges ($y = 0$ and b) may be either clamped, simply supported or free, and have no in-plane stresses. The in-plane stress of Eq. (1) acts throughout the plate and, together with the

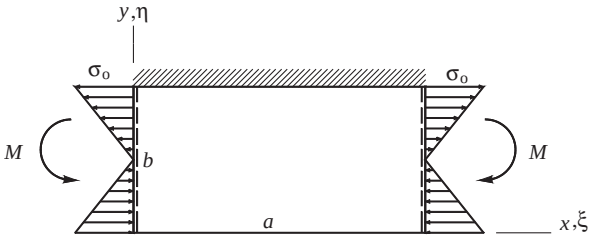

Fig. 1. An S–F–S–C rectangular plate loaded by in-plane moment, with co-ordinate convention.

other stress components $\sigma_y = \tau_{xy} = 0$, are a simple, but exact, solution of the plane elasticity problem.

Assuming that the plate is thin, has uniform thickness, and that its material is homogeneous, isotropic and linearly elastic, the equation of motion for the transverse displacement w is well known as (cf., Leissa [1])

$$D\nabla^4 w + \rho h \frac{\partial^2 w}{\partial t^2} = \sigma_x h \frac{\partial^2 w}{\partial x^2}, \tag{3}$$

where $D \equiv Eh^3/12(1-\nu^2)$ is the flexural rigidity of the plate, with E being Young's modulus, and ν being the Poisson ratio. Also, in Eq. (3) $\nabla^4 = \nabla^2\nabla^2$ is the biharmonic differential operator, with $\nabla^2 = \partial^2/\partial x^2 + \partial^2/\partial y^2$ being the Laplacian operator, ρ is mass density per unit volume, and t is time.

Introducing non-dimensional co-ordinates $\xi \equiv x/a$ and $\eta \equiv y/b$, and assuming a solution in the variables separable form

$$w(\xi, \eta, t) = Y_m(\eta) \sin m\pi\xi \sin \omega t, \tag{4}$$

Eq. (3) yields the ordinary differential equation:

$$Y_m^{\mathrm{IV}} - 2\beta_m^2 Y_m'' + \left[\beta_m^4 - 6M^*(1-2\eta)\beta_m^2 - \lambda^2\left(\frac{b}{a}\right)^4\right] Y_m = 0, \tag{5}$$

where Y_m is a function only of η, $\beta_m \equiv m\pi(b/a)$, $M^* \equiv M/D$ is the nondimensional loading parameter, and $\lambda \equiv \omega a^2\sqrt{\rho h/D}$ is the non-dimensional frequency parameter. Moreover, Eq. (4) satisfies the simply supported edge conditions of the plate exactly at $\xi = 0$ and 1.

A solution to Eq. (5) may be assumed in the form of a power series,

$$Y_m(\eta) = \sum_{n=0}^{\infty} C_{m,n}\eta^n, \tag{6}$$

which leads to the method of Frobenius. Taking derivatives of Y_m with respect to η, substituting them and Eq. (6) into Eq. (5), and shifting indices, Eq. (5) becomes

$$\sum_{n=0}^{\infty}\{[(n+4)(n+3)(n+2)(n+1)C_{m,n+4} - 2\beta_m^2(n+2)(n+1)C_{m,n+2} + \Gamma C_{m,n}]\eta^n + 12\beta_m^2 M^* C_{m,n}\eta^{n+1}\} = 0, \tag{7}$$

where

$$\Gamma \equiv \beta_m^4 - 6M^*\beta_m^2 - \lambda^2\left(\frac{b}{a}\right)^4. \tag{8}$$

Equating coefficients of like powers of η in Eq. (7), one obtains from η^0,

$$C_{m,4} = \tfrac{1}{6}\beta_m^2 C_{m,2} - \tfrac{1}{24}\Gamma C_{m,0}, \tag{9}$$

and from η^n $(n > 0)$,

$$C_{m,n+4} = \frac{2\beta_m^2(n+2)(n+1)C_{m,n+2} - \Gamma C_{m,n} - 12\beta_m^2 M^* C_{m,n-1}}{(n+4)(n+3)(n+2)(n+1)}. \tag{10}$$

Eqs. (9) and (10) are the recursion relationships for $C_{m,n}$ when $n \geqslant 4$ to the first four $C_{m,n}$.

Thus, $C_{m,0}$, $C_{m,1}$, $C_{m,2}$, and $C_{m,3}$ are arbitrary coefficients, which will be used in two boundary conditions at each side ($\eta = 0$ and 1), and the other coefficients $C_{m,n}$ for $n \geqslant 4$ are expressed in terms of them. Typically, the four boundary conditions yield four homogeneous equations with unknown $C_{m,0}$, $C_{m,1}$, $C_{m,2}$, and $C_{m,3}$. To obtain a non-trivial solution of the system, the determinant of the matrix of the coefficients is set to zero for the non-dimensional frequencies (λ). One sees that the elements of the matrix have infinite series in them. Substituting each λ back into the four homogeneous equations yields the corresponding eigenvectors, $C_{m,n}/C_{m,0}$ (with $n = 1, 2, 3$), which determines the corresponding mode shape.

There are three physically meaningful types of boundary conditions along the edges $\eta = 0$ and 1 for which this solution may be used [1]:

$$\text{clamped}: \quad w = 0 \quad \text{and} \quad \frac{\partial w}{\partial y} = 0 \Rightarrow Y_m = Y_m' = 0, \tag{11a}$$

$$\text{simply supported}: \quad w = 0 \quad \text{and} \quad M_y = 0 \Rightarrow Y_m = Y_m'' = 0, \tag{11b}$$

$$\text{free}: \quad M_y = 0 \quad \text{and} \quad V_y = 0 \Rightarrow Y_m'' = Y_m''' + m^2\pi^2(2-\nu)Y_m' = 0. \tag{11c}$$

Substituting Eq. (6) into one of the sets of boundary condition (11) for each of the two edges, $\eta = 0$ and 1, yields the fourth order characteristic determinant described earlier, from which the eigenvalues (non-dimensional frequencies) may be found. In certain special cases, the determinant quickly reduces to a lower order one.

3. Convergence study

The exact solution functions given by Eq. (6) require summing an infinite series. Depending upon the degree of accuracy which one wants to have in numerical calculations, the upper limit of the summations is truncated at a finite number (N), which may be as large as needed. This procedure is no different than that followed in the evaluation of other transcendental functions arising in the exact solutions of other boundary value problems (e.g., Bessel functions, Hankel functions).

To examine the convergence rate of the power series of Eq. (6), as well as to establish the correctness of the results, the present equations are first applied to a special case of free vibrations which has well-known, closed form solution [1,2], the *unloaded* rectangular plates with two opposites edges simply supported. In that case $M^* = 0$ in Eq. (5), resulting in constant coefficients for the ordinary differential equation, and the power series may be represented by trigonometric and hyperbolic functions of η. This convergence study is shown in Table 1.

Table 1 shows the convergence of the fundamental non-dimensional frequency parameter $\lambda \equiv \omega a^2\sqrt{\rho h/D}$ of *unloaded* rectangular plates ($a/b = 0.4$) with two opposite edges simply supported for modes having one half-wave in the x direction ($m = 1$) and $\nu = 0.3$. In the unloaded

Table 1
Convergence of the *fundamental* non-dimensional frequencies $\lambda \equiv \omega a^2\sqrt{\rho h/D}$ of *unloaded* rectangular plates with two opposite edges simply supported for $a/b = 0.4$, $m = 1$, and $v = 0.3$ by the power series method

N	S–C–S–C	S–C–S–S	S–C–S–F	S–S–S–S	S–S–S–F	S–F–S–F
5	—	—	—	—	—	6.638
6	—	—	—	11.22	11.23	4.510
7	—	—	—	11.22	11.23	7.022
8	—	—	—	11.51	11.11	6.267
9	—	—	—	11.51	11.11	7.037
10	—	—	—	11.44	10.80	6.590
11	—	—	—	11.44	10.80	7.027
12	—	—	—	**11.45**	10.58	6.678
13	—	—	—	11.45	10.58	7.032
14	—	—	—	11.45	10.40	2.632
15	0.9646	—	—	11.45	10.40	7.061
16	—	—	—	11.45	10.27	4.403
17	3.892	2.956	1.089	11.45	10.27	7.132
18	—	—	—	11.45	10.19	—
19	5.674	4.831	3.435	11.45	10.19	7.281
20	—	—	—	11.45	10.15	7.553
21	7.254	6.411	4.958	11.45	10.15	—
22	—	—	—	11.45	**10.13**	—
23	8.711	7.865	6.302	11.45	10.13	7.961
24	—	—	—	11.45	10.13	—
25	10.02	9.195	7.526	11.45	10.13	8.465
26	—	—	—	11.45	10.13	—
27	11.09	10.34	8.602	11.45	10.13	8.980
28	—	—	—	11.45	10.13	—
29	11.78	11.18	9.454	11.45	10.13	9.408
30	12.39	—	—	11.45	10.13	—
31	12.06	11.60	9.966	11.45	10.13	9.660
32	12.17	11.82	10.32	11.45	10.13	9.815
33	12.12	11.73	10.15	11.45	10.13	9.742
34	12.14	11.76	10.21	11.45	10.13	9.767
35	12.13	**11.75**	10.18	11.45	10.13	9.758
36	12.14	11.75	**10.19**	11.45	10.13	9.761
37	**12.13**	11.75	10.19	11.45	10.13	**9.760**
38	12.13	11.75	10.19	11.45	10.13	9.760
39	12.13	11.75	10.19	11.45	10.13	9.760
40	12.13	11.75	10.19	11.45	10.13	9.760
41	12.1347	11.7502	10.1888	11.4487	10.1259	9.7600
Exact	**12.1347**	**11.7502**	**10.1888**	**11.4487**	**10.1259**	**9.7600**

Notes: N total number of polynomial terms used in the power series method; the symbol (—) means that no roots were found; the non-dimensional frequencies in bold indicate the best convergent values in each column with the smallest N.

case, there are a total of six types of rectangular plates according to the edge conditions at $\eta = 0$ and 1, which are S–C–S–C, S–C–S–S, S–C–S–F, S–S–S–S, S–S–S–F, and S–F–S–F. It is seen that for even the fundamental frequencies more than 35 terms are needed to obtain the frequencies

accurately to four significant figures, with the exception of S–S–S–S and S–S–S–F plates. Table 1 also shows that as more terms are taken the frequencies converge to their exact values [2] up to six digits.

The bold numbers in the Table 1 are those beyond which the fourth digit does not change as N increases. Data are not given in Table 1 for certain small numbers of terms because of the difficulty of the computer in establishing the roots of the frequency determinant in these cases. It is also interesting to note that the convergence is not monotonic. That is, an eigenvalue (λ) oscillates about the exact value as N is increased, rather than approaching it from one direction.

Table 2 exhibits the convergence of the fundamental λ of square plates ($a/b = 1$) for modes having one half-wave in the x direction ($m = 1$) and $v = 0.3$, when the load applied is one-half of

Table 2
Convergence of non-dimensional *fundamental* frequencies $\lambda \equiv \omega a^2\sqrt{\rho h/D}$ of rectangular plates having in-plane moments acting on two opposite simply supported edges for $a/b = 1$, $m = 1$, $M/M_{cr} = 0.5$, and $v = 0.3$ by the power series method

N	S–C–S–C	S–C–S–S	S–C–S–F	S–S–S–C	S–S–S–S	S–S–S–F	S–F–S–C	S–F–S–S	S–F–S–F
7	—	—	42.69	29.38	32.86	40.53	84.80	169.5	—
8	—	—	58.80	—	—	—	—	—	—
9	158.1	204.7	129.4	15.78	10.21	7.530	3.793	—	—
10	—	—	54.39	—	—	—	—	—	—
11	—	—	23.16	53.85	56.18	59.62	6.459	4.570	160.9
12	—	—	45.33	24.64	24.11	23.33	12.09	—	—
13	198.1	204.7	63.38	15.31	13.29	13.71	8.141	6.861	4.770
14	—	—	—	8.770	—	—	9.650	9.727	—
15	—	—	54.87	74.71	75.24	76.64	8.842	7.985	6.645
16	—	—	26.62	10.78	43.37	40.92	9.186	8.694	9.121
17	253.8	256.0	45.77	20.29	20.46	22.24	9.037	8.362	7.590
18	—	—	53.54	18.11	15.14	13.78	9.096	8.496	8.110
19	—	—	102.3	20.14	20.44	92.70	9.073	8.443	7.876
20	—	—	50.31	18.13	15.24	14.12	9.081	8.462	7.964
21	18.10	7.045	27.15	19.20	17.99	18.87	**9.079**	8.455	7.931
22	—	—	21.30	18.38	16.93	16.59	9.079	8.458	7.943
23	24.49	19.20	33.34	18.95	17.28	17.30	9.079	**8.457**	7.939
24	29.31	34.78	25.93	18.88	17.09	16.90	9.079	8.457	**7.940**
25	26.74	23.65	30.34	18.92	17.21	17.14	9.079	8.457	7.940
26	27.83	26.51	28.98	18.88	17.15	17.03	9.079	8.457	7.940
27	27.32	25.04	29.05	18.92	**17.17**	17.07	9.079	8.457	7.940
28	27.53	25.63	29.24	18.90	17.17	**17.06**	9.079	8.457	7.940
29	27.45	25.38	29.09	18.91	17.17	17.06	9.079	8.457	7.940
30	27.48	25.48	29.16	18.90	17.17	17.06	9.079	8.457	7.940
31	**27.47**	25.44	**29.14**	**18.91**	17.17	17.06	9.079	8.457	7.940
32	27.47	25.46	29.14	18.91	17.17	17.06	9.079	8.457	7.940
33	27.47	**25.45**	29.14	18.91	17.17	17.06	9.079	8.457	7.940
34	27.47	25.45	29.14	18.91	17.17	17.06	9.079	8.457	7.940

Notes: N total number of polynomial terms used in the power series method; the symbol (—) means that no roots were found; the non-dimensional frequencies in bold indicate the best convergent values in each column with the smallest N.

the critical buckling value ($M/M_{cr} = 0.5$). For $M \neq 0$, all nine cases of edge conditions are distinct. M_{cr} is obtained by setting $\lambda = 0$ in Eq. (8).

4. Natural frequencies and mode shapes

Some results will now be presented which show the effects upon the plate vibration frequencies and mode shapes when the in-plane moment (M) is applied, and increased. To do this properly and meaningfully, one must first establish the critical (i.e., lowest) buckling load (M_{cr}), which is the smallest M which causes ω (and λ) to approach zero. Larger values of M are physically meaningless, and will therefore not be considered.

Table 3 shows the nondimensional critical buckling moments $M^*_{cr} \equiv M_{cr}/D$ for $\nu = 0.3$, aspect ratios $a/b = 0.5$, 1, and 2, and all nine possible edge conditions. The numbers in parentheses are the numbers of half-waves in the critical buckling mode in the x direction. Thus, for example, a square plate ($a/b = 1$) having its unloaded edges clamped has two half-sine-waves in the x direction in its critical buckling mode shape, with a node line ($x = a/2$) at its middle. The critical buckling mode shapes all have a single half-wave in the y direction; that is, no nodal lines parallel to (or approximately parallel to) the unloaded edges.

Table 4 gives fundamental frequencies $\lambda \equiv \omega a^2\sqrt{\rho h/D}$ with aspect ratios $a/b = 0.5$, 1, and 2, and $\nu = 0.3$ for unloaded plates ($M = 0$) which have all six possible combinations in edge conditions. All the fundamental frequencies have (1,1) mode shapes.

Figs. 2–4 show fundamental frequencies $\lambda \equiv \omega a^2\sqrt{\rho h/D}$ as functions of non-dimensional moment $M^* \equiv M/D$ for aspect ratios $a/b = 0.5$, 1, and 2, respectively, with $\nu = 0.3$. The values of λ shown on the ordinate are the non-dimensional fundamental frequencies for no loading ($M = 0$), which are listed in Table 4. The values of M^* for $\lambda = 0$ shown on the abscissa are the non-dimensional critical buckling moments, which are given in Table 3.

Fig. 2 shows that the fundamental free vibration mode shapes for $a/b = 0.5$ all have (1,1) mode shapes, irrespective of M/D and edge conditions. Fig. 3 describes how, as M approaches the

Table 3
Non-dimensional critical buckling moments $M^*_{cr} \equiv M_{cr}/D$ ($\nu = 0.3$)

Edge conditions	a/b		
	0.5	1	2
S–C–S–C	65.26 (1)	65.26 (2)	65.26 (4)
S–C–S–S	65.26 (1)	65.26 (2)	65.26 (4)
S–C–S–F	65.24 (1)	65.24 (2)	65.24 (4)
S–S–S–C	42.00 (1)	42.00 (2)	39.38 (3)
S–S–S–S	41.99 (1)	41.99 (2)	39.28 (3)
S–S–S–F	41.98 (1)	41.98 (2)	39.24 (3)
S–F–S–C	11.64 (1)	4.591 (1)	3.646 (1)
S–F–S–S	11.63 (1)	4.327 (1)	2.181 (1)
S–F–S–F	11.63 (1)	4.289 (1)	1.876 (1)

Note: numbers in parentheses are the numbers of half-waves (m) in the buckling mode in the x direction.

Table 4
Non-dimensional fundamental frequencies $\lambda \equiv \omega a^2\sqrt{\rho h/D}$ for *unloaded* plates ($\nu = 0.3$)

Edge conditions	a/b		
	0.5	1	2
S–C–S–C	13.69	28.95	95.26
S–C–S–S or S–S–S–C	12.92	23.65	69.33
S–C–S–F or S–F–S–C	10.43	12.69	22.82
S–S–S–S	12.34	19.74	49.35
S–S–S–F or S–F–S–S	10.30	11.68	16.13
S–F–S–F	9.736	9.631	9.512

Note: All frequencies have (1,1) mode shapes.

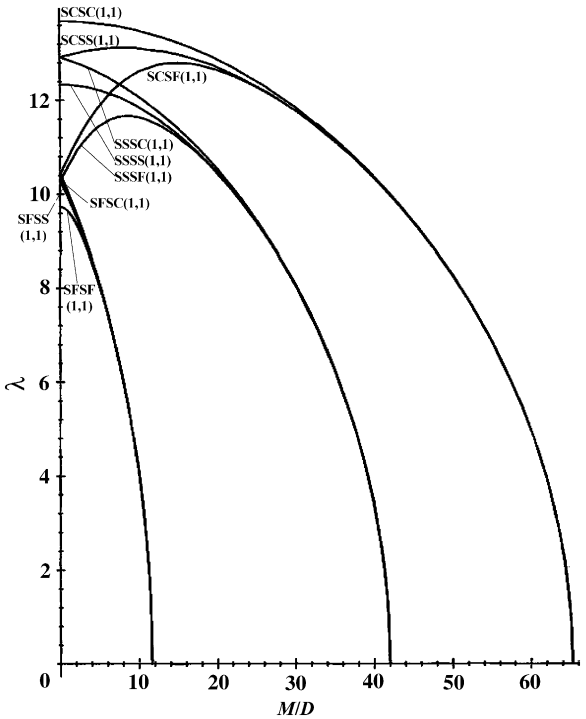

Fig. 2. Fundamental frequencies $\lambda \equiv \omega a^2\sqrt{\rho h/D}$ as functions of non-dimensional moment ($\equiv M/D$) for $a/b = 0.5$ and $\nu = 0.3$.

critical buckling moments, the fundamental free vibration mode shapes for square plates ($a/b = 1$) change from (1,1) to (2,1) modes, except for S–F–S–C, S–F–S–S, and S–F–S–F plates, for which the fundamental ones are (1,1) irrespective of M. For relatively long plates ($a/b = 2$), the fundamental mode shapes change even more drastically, as seen in Fig. 4. For example, for S–S–S–C, S–S–S–S, and S–S–S–F plates, the fundamental mode shape changes from (1,1) to (2,1) to (3,1) as M increases. It is very interesting to note that the fundamental free vibration mode

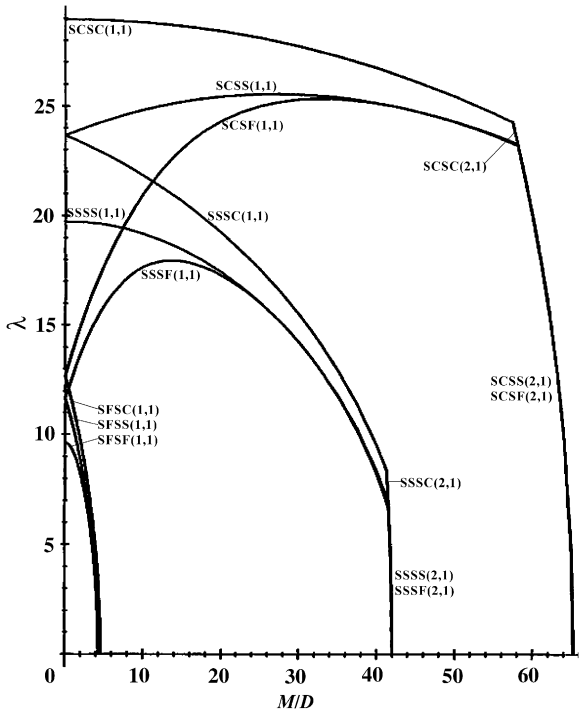

Fig. 3. Fundamental frequencies $\lambda \equiv \omega a^2\sqrt{\rho h/D}$ as functions of non-dimensional moment M^* ($\equiv M/D$) for $a/b = 1$ and $\nu = 0.3$.

shapes move from (1,1) directly into (4,1) not via (2,1) and (3,1) for S–C–S–S and S–C–S–F plates. In the case of the S–C–S–C plate, the modes go from (1,1) to (3,1) and then (4,1), skipping the (2,1) mode. In these cases the skipped modes exist, but they correspond to higher frequencies.

Particularly interesting in Figs. 2–4 is the fact that initially, as M is applied, the fundamental frequencies of the S–C–S–S, S–C–S–F and S–S–S–F plates *increase*, instead of decrease, even though one-half of the plate is in compression. Typically, the presence of compressive in-plane stresses destabilizes a plate, causing frequencies to decrease, but these are exceptions. For these three sets of edge conditions, the *more constraining* of the two unloaded edges ($y = 0$, see Fig. 1) is in compression. Nevertheless, as Figs. 2–4 show, although applying M causes the fundamental frequencies to increase initially, eventually they decrease with larger M.

To understand better the curve crossing of Figs. 3 and 4, Fig. 5 is added, which shows the first *five* frequency parameters (λ/π^2) versus non-dimensional moment (M/D) for an S–S–S–S square plate ($a/b = 1$). For no loading ($M = 0$), the first five frequencies correspond to (1,1), (1,2) or (2,1), (2,2), and (3,1) mode shapes, in that order, in which the frequencies for the (1,2) and (2,1) modes are degenerated. As M is applied, the frequencies for the modes of (1,1), (2,1), and (3,1) decrease, but the ones for the other modes (1,2) and (2,2) increase slightly. Eventually, as M is increased further, the (2,1) frequency curve crosses the (1,1) curve, and the plate buckles in a (2,1) mode. The (1,1) and (3,1) modes have a higher buckling moments. The (1,2) and (2,2) frequencies also decrease (beyond the abscissa limit of Fig. 5) and eventually go to zero at a large value of M/D.

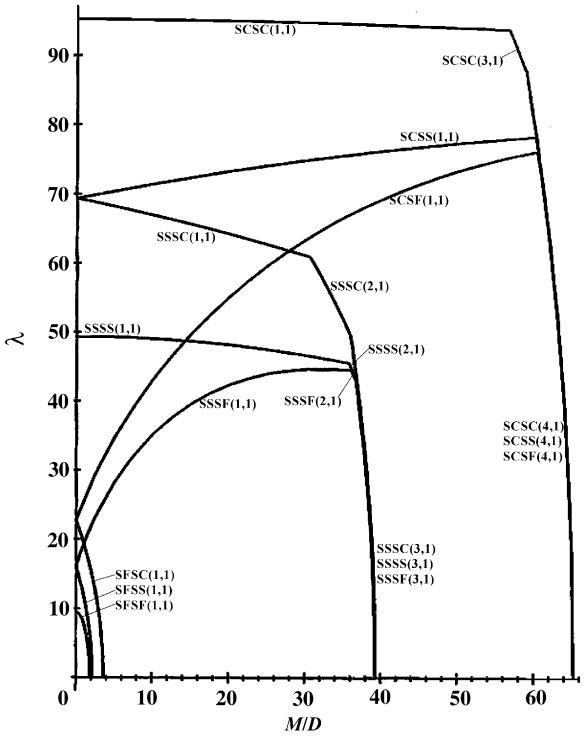

Fig. 4. Fundamental frequencies $\lambda \equiv \omega a^2\sqrt{\rho h/D}$ as functions of non-dimensional moment M^* ($\equiv M/D$) for $a/b = 2$ and $v = 0.3$.

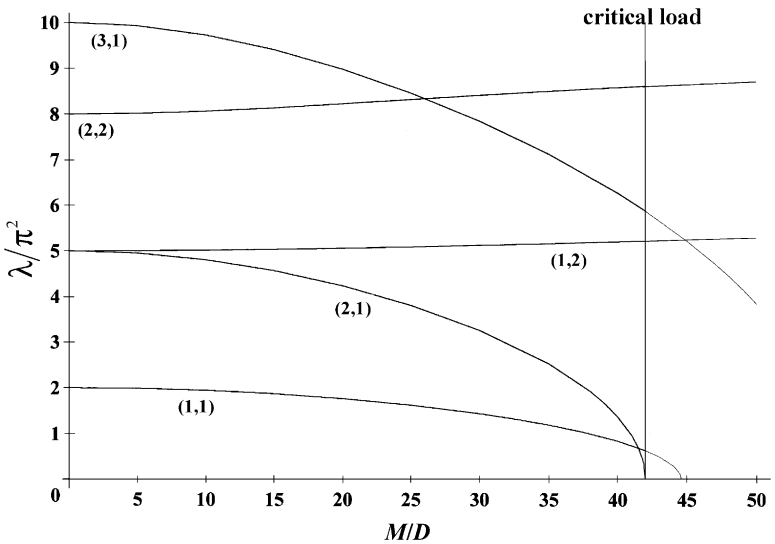

Fig. 5. Frequency parameter λ/π^2 vs. non-dimensional moment M/D for an S–S–S–S square plate ($a/b = 1$).

Contour plots of the free vibration mode shapes of square plates ($a/b = 1$) for all nine possible boundary conditions are seen in Figs. 6–8, with end moments $M/M_{cr} = 0$, 0.5, 0.95 applied and $v = 0.3$. Again, M_{cr} is the critical buckling moment for each plate, found in Table 3. Figs. 6–8 correspond to the first, second, and third free vibration mode shapes, respectively. The maximum displacements of all the plots are marked with $\times$.

The contour plots of the first column in Fig. 6 correspond to the frequencies listed in the second column of Table 4 for unloaded plates ($M = 0$), where all the fundamental frequencies have (1,1) mode shapes. The contour plots of the third column for $M/M_{cr} = 0.95$ in Fig. 6 show that as M approaches M_{cr}, the first free vibration mode shapes approach the critical buckling mode shapes listed in the second column of Table 3, except for S–S–S–C, S–S–S–S, and S–S–S–F, where their critical buckling mode shapes are for (2,1) modes, instead of the (1,1) modes observed in Fig. 6.

It is interesting to note how the contour lines shift downward (i.e., towards the compressive lateral plate edge) as the end moment M is increased. For the (1,1), (2,1), and (3,1) modes, the point of maximum displacement moves towards the compressive region of the plate. For the (1,2) and (1,3) modes, the nodal lines also shift downward (see, for example, the (1,2) mode for the S–S–S–F plate in Figs. 7 and 8).

The movement of the mode shape contour lines and the point of maximum displacement downward towards the compressive regions is seen most dramatically for the three cases (S–C–S–S, S–C–S–F, S–S–S–F) where increasing moment initially increases the fundamental frequencies. The identifying symbols for these three cases are underlined in Fig. 6. Studying Fig. 6 carefully, one observes that only for these three cases is the point of maximum displacement towards the upper plate edge when no moment is applied ($M/M_{cr} = 0$). But these are also the only three cases where the upper edge is less constrained than the lower edge. The downward movement is demonstrated in Fig. 9, where the edge moments are increased gradually on an S-S-S-F square plate. As could be expected, with $M/M_{cr} = 0$ the maximum displacement is in the middle of the upper edge, which is free. As moment is applied and increased, the point of maximum displacement moves downward toward the compression region, crossing into it when $M/M_{cr} < 0.5$.

5. Concluding remarks

The foregoing work has shown how an exact procedure may be followed to analyze the free vibrations of rectangular plates having two opposite edges simply supported, with those edges being subjected to linearly varying normal stresses causing pure in-plane moments. The procedure was applied to all possible combinations of clamped, simply supported or free edge conditions applied continuously along the other two edges. Additional, extensive results for the S–F–S–F [3] and S–C–S–C [4] plates are also available elsewhere.

Assuming a sinusoidal displacement in the x direction resulted in a separation of variables (x and y), yielding an ordinary differential equation in y which had variable coefficients. An exact solution of this was obtained in terms of an infinite power series. The infinite series thus generated represent transcendental functions in the same manner as other commonly used functions (e.g., trigonometric, hyperbolic, Bessel, Hankel) which are also evaluated by power series, except that present ones have no "name" assigned to them. Thus, for example, well-known [1,2] exact

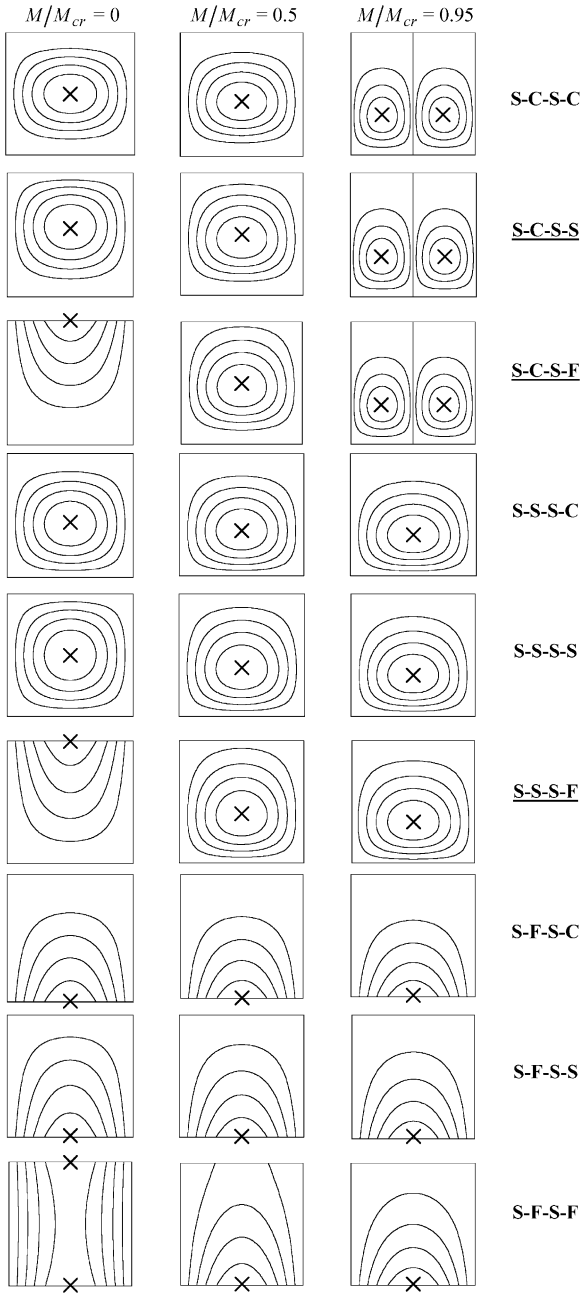

Fig. 6. Free vibration *fundamental* mode shapes of square plates ($a/b = 1$) with in-plane pure bending for $\nu = 0.3$. (Maximum displacements marked with $\times$.)

solutions for the frequencies of rectangular plates having two opposite edges simply supported, *without* in-plane forces, use trigonometric and hyperbolic functions for $Y(\eta)$ in Eq. (6). Applying boundary conditions (11) at the two other edges yields a fourth order determinant, the elements of

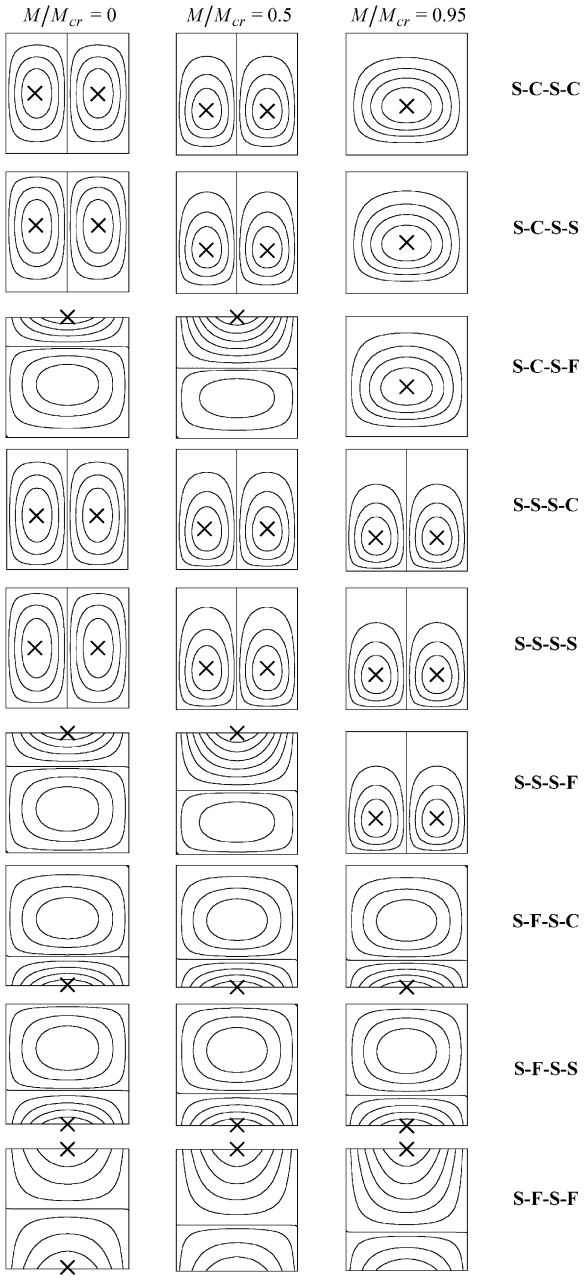

Fig. 7. Free vibration *second* mode shapes of plates with in-plane pure bending for $a/b = 1$ and $v = 0.3$. (Maximum displacements marked with $\times$.)

which are $Y(\eta)$ and/or its derivatives, as in the present problem. The computer evaluating the trigonometric or hyperbolic functions and their derivatives does so by summing the power series for these functions. Similarly, well-known exact solutions for circular plates [1] use ordinary and

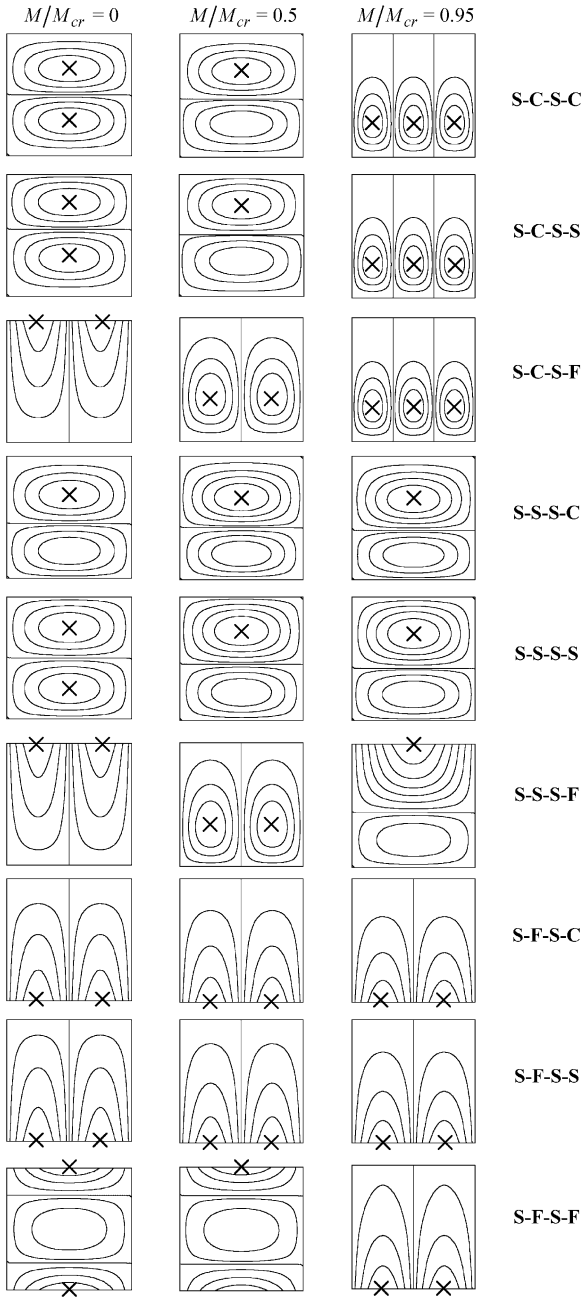

Fig. 8. Free vibration *third* mode shapes of plates with in-plane pure bending for $a/b = 1$ and $v = 0.3$. (Maximum displacements marked with $\times$.)

modified Bessel functions and their derivatives as elements of the frequency determinant, and these functions are evaluated by summing truncations of infinite power series. As it was shown in the present work, care must be taken to use a sufficient number of terms of the series to obtain

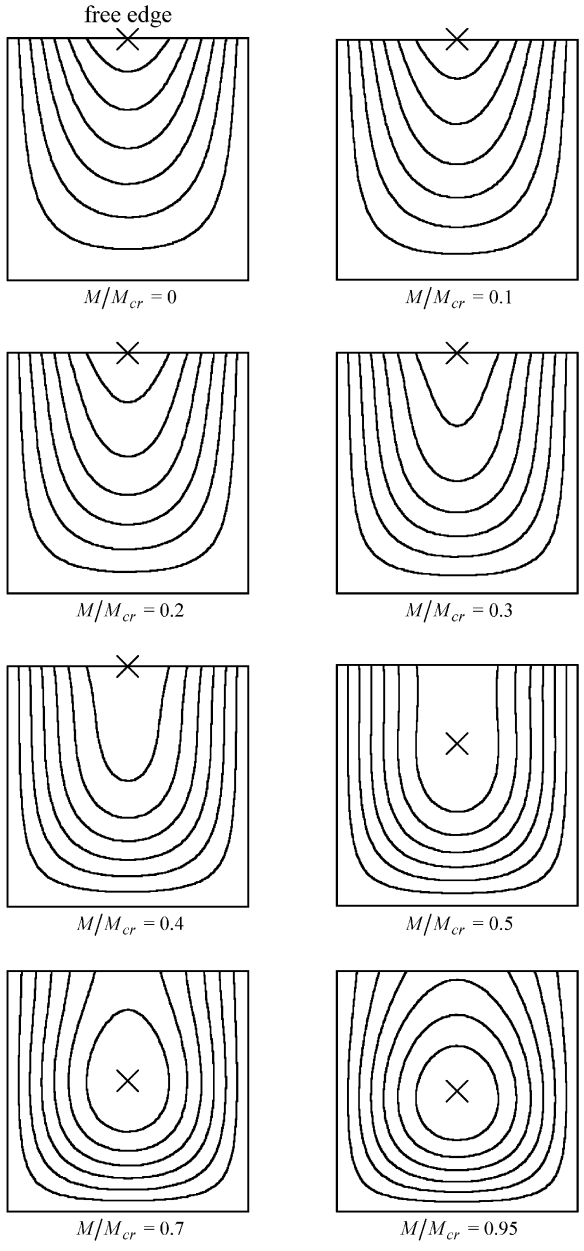

Fig. 9. Movement of fundamental mode contour lines with increasing edge moment on an S–S–S–F square plate for $\nu = 0.3$. (Maximum displacements marked with $\times$).

accurate numerical results. This, of course, is a consideration when evaluating any functions expressed as an infinite series.

The convergence of the series, as displayed for example in Tables 1 and 2, is particularly interesting. It was demonstrated that reasonably accurate results *cannot* be obtained by simply

taking a few terms of the series. Indeed, for these examples at least 20 terms were needed (except for unloaded S–S–S–S plate), and typically more than 30. Also notable was the relatively wild character of the convergence. It is not monotonic, but oscillatory. Moreover, the oscillation amplitude does not necessarily decrease term-by-term as terms are added. Most astonishingly, solutions could not even be established numerically for small numbers of terms because of the extreme oscillation then present. However, as Tables 1 and 2 show, as sufficient terms of the polynomials are used, the series and frequencies converge correctly, and exactly.

Some previous results have appeared for the buckling case, which is a special case of the free vibration problem for the loaded plate, obtained by the method of energy or the method of integration of the differential equation. However, no other results are known for free vibration problem, except for those recently published for the S–F–S–F [3] and S–C–S–C [4] plates.

Also very interesting is that Figs. 2–4 demonstrate that for three of the nine cases, the fundamental frequency of the rectangular plates is initially *increased* as in-plane bending moment is applied. This may be surprising, because one-half of the stress causing the moment is compressive, and compressive stresses typically decrease frequencies. And it is well known that large in-plane moments will cause severe decreases in frequencies, approaching zero when the plate buckles. The authors are unaware of any other results in published literature which show an initial increase in a plate fundamental frequency when compressive stress is applied.

The present study was limited to plates having linearly varying in-plane stresses applied to the simply supported edges, their resultants being in-plane pure *moments* (couples), with no resultant *forces*. The method used could have been applied equally well to more general linear stress variations. However, one cannot generalize this statement to other polynomial variations of σ_x with y along the edges $x = 0$ and a, because the resulting stress components within the plate (determined from a plane elasticity solution) would result in all three stress components $(\sigma_x, \sigma_y, \tau_{xy})$ being functions of *both* x and y, and an exact, variables separable solution of the free vibration problem would be intractable.

Acknowledgements

This research was supported by the University of Chung-Ang Special Research Grants in 2002.

The authors thank Professor Arthur W. Leissa for his careful review of the manuscript, continuous encouragement, and valuable advice.

References

[1] A.W. Leissa, *Vibration of Plates*, NASA SP 160, US Government Printing Office, 1969; reprinted 1993 by the Acoustical Society of America.

[2] A.W. Leissa, The free vibration of rectangular plates, *Journal of Sound and Vibration* 31 (1973) 257–293.

[3] J.-H. Kang, A.W. Leissa, Vibration and buckling of SS–F–SS–F rectangular plates loaded by in-plane moments, *International Journal of Structural Stability and Dynamics* 1 (4) (2001) 527–543.

[4] A.W. Leissa, J.-H. Kang, Exact solutions for vibration and buckling of an SS–C–SS–C rectangular plate loaded by linearly varying in-plane stresses, *International Journal of Mechanical Sciences* 44 (9) (2002) 1925–1945.